UNIVERSIDADE DE LISBOA
FACULDADE DE CIÊNCIAS
DEPARTAMENTO DE BIOLOGIA ANIMAL

Unveiling myosin dysfunction in Hypertrophic Cardiomyopathy

Débora Trogeira Cruz

Mestrado em Biologia Humana e Ambiente

Dissertação orientada por:
Professor Assistente Julien Ochala, Universidade de Copenhaga
Professora Maria Teresa Rebelo, Universidade de Lisboa

2023

Resumo

O ventrículo esquerdo impulsiona o sangue para todo o corpo durante a contração dos cardiomiócitos, que são constituídos por feixes de miofibrilas que contêm miofilamentos, onde se podem encontrar os sarcómeros. Estes miofilamentos são compostos por filamentos finos (actina) e grossos (miosina). As miosinas têm dois estados de repouso: o estado desordenado-relaxado (DRX) e o estado super-relaxado (SRX). DRX é um estado em que uma cabeça globular está disponível para se ligar à actina. No estado SRX, as cabeças globulares estão ligadas entre si e à cauda da miosina. As miosinas não participam na contração mas em caso de maior necessidade mecânica, fornecem cabeças globulares de reserva que podem ser ativadas. Neste estado, uma vez que as cabeças de miosina estão ligadas umas às outras ao longo do filamento grosso, o estado de SRX apresenta uma taxa de renovação de ATP altamente inibida.

Cardiomiopatia hipertrófica (CMH) é a doença genética cardíaca mais prevalente, levando à morte súbita cardíaca precoce, afetando mais de 1 em cada 500 pessoas em todo o mundo. Esta doença é caracterizada por um espessamento da parede do ventrículo esquerdo, resultando numa redução do fornecimento de sangue ao corpo e numa pressão elevada na aurícula esquerda. Metade dos casos de CMH são causados por mutações em genes que codificam proteínas presentes nos sarcómeros (mutação sarcomérica positiva - MSP), e a outra metade apresentam causas não identificadas (mutação sarcomérica negativa - MSN).

As principais mutações em MSP encontram-se em genes que codificam proteínas como MYH7 e MYBPC3, que codificam a cadeia pesada da β-miosina e a proteína C de ligação à miosina, respetivamente. A maioria das variantes de CMH em MYBPC3 codificam truncações que promovem uma mudança na quantidade de miosinas no estado DRX, aumentando a contratilidade da miosina.

Supõe-se que os estados SRX e DRX estejam em equilíbrio, sendo que a desregulação do estado SRX em condições cardíacas hereditárias ou adquiridas pode influenciar a função contrátil do cardiomiócito. Na CMH, as mutações da miosina podem promover uma mudança no equilíbrio que pode resultar em mais cabeças da miosina disponíveis para interagir com a actina, o que pode explicar a hipercontratilidade observada clinicamente.

As características moleculares da MSP-CMH incluem a hiper-contratilidade devido ao excesso de ligações miosina-actina e à desregulação do estado super-relaxado da miosina (SRX).

Mavacamten (MYK-461) é um inibidor alostérico e reversível de pequenas moléculas da miosina ATPase cardíaca que normaliza a hipercontratilidade do sarcómero ligando-se diretamente à miosina, o que inibe a formação excessiva de pontes cruzadas de miosina e actina e promove o estado SRX na miosina. É um fármaco em investigação que pode interromper o desenvolvimento da hipertrofia e das complicações clínicas observadas na CMH.

O objetivo desta dissertação foi analisar se o equilíbrio SRX-DRX está alterado, levando assim a um consumo excessivo de ATP, em amostras de pacientes com CMH com MSP e MSN e investigar se a adição de MYK-461 restaura o equilíbrio SRX-DRX.

O método de perseguição com MANT-ATP foi efetuado de modo a determinar a distribuição de SRX/DRX. Trata-se de um método quantitativo de microscopia de epi-fluorescência, em que os nucleótidos de MANT se ligam à miosina para medir o equilíbrio SRX-DRX. O MANT-ATP é um análogo do ATP que altera significativamente a sua intensidade de emissão quando ligado à miosina, apresentando um aumento da emissão de fluorescência. Quando se perde a associação entre a miosina e o MANT-ATP, verifica-se uma diminuição da fluorescência. As alterações da fluorescência permitem medir a ligação e a dissociação do MANT-ATP. O método de perseguição de MANT-ATP foi aplicado com e sem MYK-461 nas diferentes amostras, de forma a medir o tempo de rotaçao da miosina entre DRX e SRX.

A fim de testar os objetivos desta dissertação, foram utilizadas neste estudo quinze miectomias humanas. Todas as amostras eram provenientes de cirurgias de miectomia que removeram parte do septo do ventrículo esquerdo para aliviar a obstrução da válvula. Uma das amostras era de um dador, sete eram de MSP e sete eram de MSN. Nas amostras com MSP, duas apresentavam uma mutação MYH7 e as restantes cinco apresentavam uma mutação MYBPC3.

Foram realizadas quatro lâminas para cada amostra, duas com mavacamten e duas sem este. Para cada lâmina, foram dissecadas 6 tiras cardíacas, o que significa que foram montadas 24 tiras cardíacas para cada amostra. O método de perseguição MANT-ATP foi efetuado em todas as lâminas e em seguida todos os dados foram analisados usando os programas Image J e GraphPad Prism. Foram realizados testes estatísticos tendo em conta dois fatores: grupo (dadores vs MSP vs MSN) e tratamento (com MYK-461 vs sem MYK-461). Os resultados obtidos do processo de decaimento em duas fases foram calculados como média para cada grupo específico. Para analisar os dados, foi efetuada uma Two-Way ANOVA utilizando o programa GraphPad Prism 9.0, seguida de uma análise post hoc de Tukey. A significância estatística foi considerada significativa com um limiar de $p<0,05$, para testar se as amostras cardíacas apresentavam uma distribuição diferente de DRX/SRX com e sem mavacamten.

Ao comparar as amostras de CMH com a amostra de dador através da interpretação dos resultados estatísticos da análise de P1 (índice para DRX), é possível deduzir que existe uma diferença significativa na percentagem de DRX, entre as amostras de MSP, MSN e dador.

Os resultados indicaram que não houve uma variação estatisticamente significativa no rácio SRX-DRX em todos os grupos, após ter sido adicionado MYK-461. No entanto, ao comparar a média de cada grupo, é possível avaliar que o tratamento com MYK-461 tendeu a baixar P1 e a aumentar P2 (índice para SRX) nos doentes com MSP, em contraste com os dadores e os doentes com MSN. Verifica-se também que a percentagem de miosina no estado SRX é mais elevada na amostra do dador do que nos doentes com CMH.

Ao comparar a média de cada amostra, verifica-se que a percentagem de miosina no estado SRX é mais elevado na amostra de dadores do que na de doentes com CMH. Além disso, ao comparar todos os valores de P1, é notável que os doentes com MSP tendem a ter um valor de P1 mais elevado (maior percentagem de DRX), em comparação com os dadores ou doentes com mutações MSN.

Tal como observado no decaimento exponencial, as amostras com MSP apresentaram um decaimento muito mais rápido, em contraste com as amostras de dadores e de MSN.

Este estudo apresentou diversas limitações, incluindo um número restrito de doentes, o que levou a um conjunto de dados limitado. Além disso, os métodos empregues consumiram muito tempo, tornando impraticável a recolha de um tamanho de amostra maior devido ao extenso tempo que é necessário para a experimentação de cada amostra individual.

A dimensão da amostra do estudo de quinze pessoas pode não ter proporcionado poder estatístico suficiente para detetar alterações significativas após a aplicação do MYK-461. Por conseguinte, é aconselhável incluir um maior número de amostras em análises futuras para aumentar a fiabilidade dos resultados.

CMH é a doença cardíaca genética mais prevalente, sendo portanto notável a importância de encontrar um fármaco que atue ao nível de todas as mutações potenciadores deste distúrbio. Tendo isto em conta, a próxima fase da investigação de CMH – MSN deve envolver alterações a nível dos reagentes utilizados na preparação da amostra e também na concentração de mavacamten utilizada.

PALAVRAS-CHAVE: Cardiomiopatia hipertrófica (CMH), Mavacamten (MYK-461), Mutação Sarcomérica Positiva (MSP), Mutação Sarcomérica Negativa (MSN), Miosina.

Abstract

Hypertrophic cardiomyopathy (HCM) is the most prevalent cardiac genetic disease, often leading to early sudden cardiac death, affecting more than 1 in 500 people worldwide. This condition is characterized by a thickened left ventricular wall, resulting in reduced blood supply to the body and elevated pressure in the left atrium. Half of HCM cases are caused by mutations in genes encoding sarcomeric proteins (sarcomere mutation-positive cases - SMP), and the other half cases have unidentified causes (sarcomere mutation-negative cases - SMN).

Molecular features of SMP-HCM include hyper-contractility as attested by an excess myosin cross-bridge formation and dysregulation of myosin super-relaxed state (SRX).

Mavacamten (MYK-461), a small molecule that lowers hyper-contractility by inhibiting myosin ATPase activity, has been proven efficient in SMP-HCM. It reduces myosin cross-bridge numbers and promotes myosin SRX state.

The aim of this dissertation was to analyse if the SRX-DRX equilibrium was altered, thereby leading to an over-consumption of ATP, in samples from SMP and SMN patients with HCM and to investigate if the addition of MYK-461 restores de SRX-DRX equilibrium.

Myectomy samples from SMP-HCM patients, SMN-HCM patients, and healthy donors were used. The MANT-ATP chase experiment was applied with and without MYK-461 to measure the myosin turnover.

The results showed a significant difference in P1 and P2 between the groups of samples (SMP, SMN and donors), but not between treatment with MYK-4611. However, SMP patients tend to have a higher P1 compared to donors or patients with SMN mutations. Treatment with MYK-461 tended to lower P1 and increase P2 for SMP patients in contrast to donors and patients with SMN mutations. From these results can it be concluded that MYK-461 did not make a substantial difference.

A small sample size might be the cause, thus more myectomy samples need to be analyzed.

KEYWORDS: Hypertrophic Cardiomyopathy (HCM), Mavacamten (MYK-461), Sarcomere Mutation-Positive (SMP), Sarcomere Mutation-Negative (SMN), Myosin.

List of Contents

Resumo 1
Abstract 3
List of Contents 4
List of Figures and Tables 5
List of Abbreviations 6
1. Introduction 7
1.1 Heart Function 7
1.2 Cardiomyocyte Function 8
1.3 Sarcomere Structure 8
1.4 Muscle Contraction 11
1.5 Myosin Conformations 11
1.6 Hypertrophic Cardiomyopathy (HCM) 13
1.7 Mavacamten 14
2. Hypothesis And Objectives 15
3. Material And Methods 16
3.1 Cardiac Tissue 16
3.2 Storage Of The Tissue 17
3.3 Sample Preparation 17
3.4 The MANT-ATP Chase Experiment 18
3.5 Quantification And Statistical Analysis 19
4. Results 20
4.1 Analyse If The SRX-DRX Equilibrium Is Altered 20
4.2 Investigate If The Addition Of Mavacamten (MYK-461) Restores The SRX-DRX Equilibrium 21
4.3 Compare The SRX-DRX Equilibrium Between The HCM Patients And The Healthy Donors 23
4.4 Other Results 25
5. Discussion 26
6. Conclusion 28
7. References 29
8. Appendix 33

List of Figures and Tables

Figure 1.1.1 - Layers of the heart (Betts et al., 2022) ……...……..7
Figure 1.3.1 - Schematic of sarcomere structure (Santiago et al., 2021). …….…..8
Figure 1.3.2 - Cardiac myosin structure. Yellow and green represent heavy chains, each bound to an essential light chain and a regulatory light chain. The S1 region corresponds to the myosin heads. Light meromyosin is the tail region and heavy meromyosin is the globular head region. The myosin tail (light meromyosin) assembles into the tick filament (Barrick & Greenberg, 2021)……10
Figure 1.3.3 – When the contraction of the sarcomere occurs, the Z lines move closer, resulting in a reduction of the I band's size (Betts et al., 2022)……10
Figure 1.5.1 – Illustration of the super-relaxed state and the disordered-relaxed state. In the super-relaxed state, the myosin heads are bound to the thick filament, while in the disordered-relaxed state they are free (Barrick & Greenberg, 2021)…….…….....12
Figure 1.6.1 - Illustration of the differences between a healthy hearth and a hearth with hypertrophic cardiomyopathy (Mayo Clinic, 2022)……..……13
Figure 1.7.1 – Effect of Mavacamten on myosin (Pysz et al., 2021) ……14
Table 3.1.1 - Available information on the patients, their mutation, gender, age, Body Mass Index (BMI) and Left Ventricule (LV) ejection fraction……16
Figure 3.3.1 – Illustration of the process of cutting grids for the MANT-ATP chase experiment (Created with Biorender). ……17
Figure 3.3.2 – Cardiac strips mounted onto the copper grids. The last picture is the slide fully prepared for the MANT-ATP chase experiment, with the flow chamber (Original photography). ……..18
Figure 4.1.1 and 4.1.2 - Plots showing the mean of P1 (index od DRX) and P2 (index of SRX) from each sample without mavacamten, as larger colored figures……...20
Figure 4.2.1 and 4.2.2 - Super plots showing all single fibers used in the Mant-ATP chase experiment presented as small light gray figures and the mean of each sample as larger colored figures. Plot of P1 (index of DRX), where the initial rapid decay correspondes to DRX. Plot of P2 (index of SRX), where the slow decay correspondes to SRX……..…….21
Table 4.2.1 – P1 statistical results from the 2way ANOVA…….....21
Table 4.2.2 – P2 statistical results from the 2way ANOVA…….....21
Figure 4.2.3 and 4.2.4 – Super plots showing all single fibers used in the Mant-ATP chase experiment presented as small light gray figures and the mean of each sample as larger colored figures. Plot of T1 (index of DRX ATP turnover time) and plot of T2 (index of SRX ATP turnover time)……..……....22
Table 4.2.3 – T1 statistical results from the 2way ANOVA……..22
Table 4.2.4 – T2 statistical results from the 2way ANOVA……..22
Table 4.3.1 - Summarizes the mean ±S.E.M. for P1 (index of DRX), P2 (index of SRX), T1 (index of DRX ATP turnover time), and T2 (index of SRX ATP turnover time) for all the strips that were included……23
Table 4.3.2 - The average P1 (index of DRX), P2 (index of SRX), T1 (index of DRX ATP turnover time), and T2 (index of SRX ATP turnover time) from the results in table 4.3.1…….....24
Figure 4.4.1 - Mant-ATP fluorescence decay caused by flushing with ATP. Data are fit by a double exponential decay to assess the DRX-SRX ratio……...25

List of Abbreviations

ADP - Adenosine Diphosphate
ATP - Adenosine 5'-triphosphate
BMI - Body Mass Index
Ca^{2+} - Calcium
cMyBP-C - Cardiac myosin binding protein-C
DCM - Dilated Cardiomyopathy
DRX - Disordered-Relaxed State
EF - Ejection Fraction
ELC - Essential Light Chains
F-actin - Filamentous actin
HCM - Hypertrophic Cardiomyopathy
HMM- Heavy Meromyosin
IHM - Interacting-Heads Motif
LV - Left Ventricle
LVOT - Left Ventricular Outflow Tract
MANT-ATP - 2'-(or-3')-O-(N-Methylanthraniloyl)-Adenosine-5'-Triphosphate, trisodium Salt
MyHC - Myosin Heavy Chains
MYK-461 - Mavacamten
P1 - Index of DRX
P2 - Index for SRX
Pi - Inorganic Phosphate
RLC - Regulatory Light Chains
S1 - Subfragment 1
S2 - Subfragment 2
SMN - Sarcomere Mutation Negative
SMP - Sarcomere Mutation Positive
SRX - Super-Relaxed State
T1 - Index of DRX ATP turnover time
T2 - Index of SRX ATP turnover time
Tm - Tropomyosin
Tn - Troponin
TnC - Troponin-C

1. Introduction

1.1 Heart Function

The human heart is composed of four chambers, separated by the septum. Each side consists of one atrium and one ventricle. The atria, located in the upper portion of the heart, act as receiving chambers. They contract to propel blood into the lower chambers, known as the ventricles. The ventricles, situated in the lower portion of the heart, serve as the primary pumping chambers (Betts et al., 2022). The heart efficiently circulates blood and essential nutrients to all organs, ensuring their proper functionality. The synchronized contraction creates the necessary pressure to propel blood through arteries, reaching even the farthest organs. This consistent and rhythmic pumping action sustains circulation to all vital body parts (Voorhees & Han, 2015).

The wall of the heart comprises three layers of varying thickness. Progressing from superficial to deep, these layers are known as the epicardium, the myocardium, and the endocardium (Figure 1.1.1). The middle layer, recognized as the myocardium, holds the distinction of being the thickest layer. It primarily consists of cardiac muscle cells (cardiomyocytes) forming the foundation of its structure. Additionally, the myocardium is supported by a framework of collagenous fibers, along with blood vessels and nerve fibers that contribute to regulating the heart's activity (Betts et al., 2022).

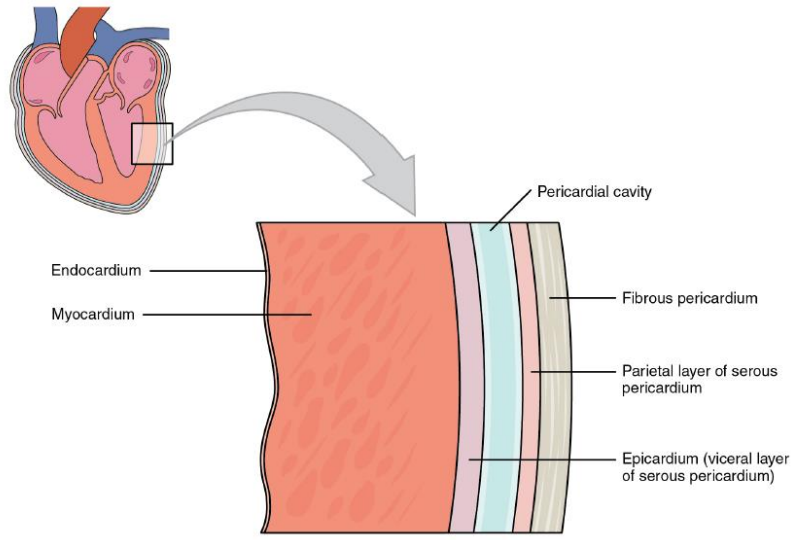

Figure 1.1.1 – Layers of the heart (Betts et al., 2022).

The left ventricle (LV) possesses the essential role of propelling blood to the distal organs and all the body's extremities. Heart failure arises when the left ventricle becomes incapable of meeting the body's demands. The overall performance of the pump is contingent upon several factors, including the force of contraction exhibited by the myocardium, the prevailing loading conditions, the size and shape of the ventricle, and the proper function of the valves, among other considerations. These elements play crucial roles in determining the effectiveness and efficiency of the pump's operation (Voorhees & Han, 2015).

The heart function can be described by the ejection fraction (EF) and commonly falls within the range of 50 to 80%. Readings below this range indicate a potential sign of heart failure (Voorhees & Han, 2015).

1.2 Cardiomyocyte Function

The middle layer of the heart, known as the myocardium, is composed of cardiomyocytes, which are cardiac muscle cells (Voorhees & Han, 2015).

A cardiomyocyte assumes the crucial responsibility of facilitating the heart's contraction, possesses a high density of mitochondria and are subject to involuntary sympathetic control (Keepers et al., 2020). Each individual myocyte possesses a single nucleus, located centrally within the cell, and is encompassed by a cell membrane referred to as the sarcolemma. Notably, the sarcolemma of cardiac muscle cells contains specialized ion channels and voltage-gated calcium channels that store and provide calcium for the contraction. Cardiac muscle cells are composed of branched fibers that are interconnected through intercalated discs, housing both gap junctions and desmosomes. This intricate network of interconnections enables the cardiomyocytes to contract collectively and in synchronization, facilitating the heart's efficient pumping action (Ripa et al., 2023).

1.3 Sarcomere Structure

The sarcomere, which serves as the basic unit of contraction in cardiomyocytes, is notably comprised of thick (myosin) and thin (actin) filaments (Ripa et al., 2023).

Thin filaments made of actin together with thick filaments containing myosin, interconnect in the middle of the sarcomere (Crocini & Gotthardt, 2021). Muscle contraction is the result of thick and thin filaments sliding onto each other.

The ends of each sarcomere are defined by the Z disc. Within each sarcomere, A bands containing thick (myosin) filaments, alternate with I bands that only contain thin (actin) filaments. In the middle of the sarcomere, the myosin filaments are anchored at the M-line and the actin filaments are attached to the Z-disc (Figure 1.3.1). Extending between the Z disc and the thick filament is the elastic filament, titin, which serves as the central component of the thick filament (Irving, 2012). When the muscle contracts, each sarcomere shortens, bringing the Z discs closer together, and the actin filaments move into the A band and H zone (Cooper, 2000).

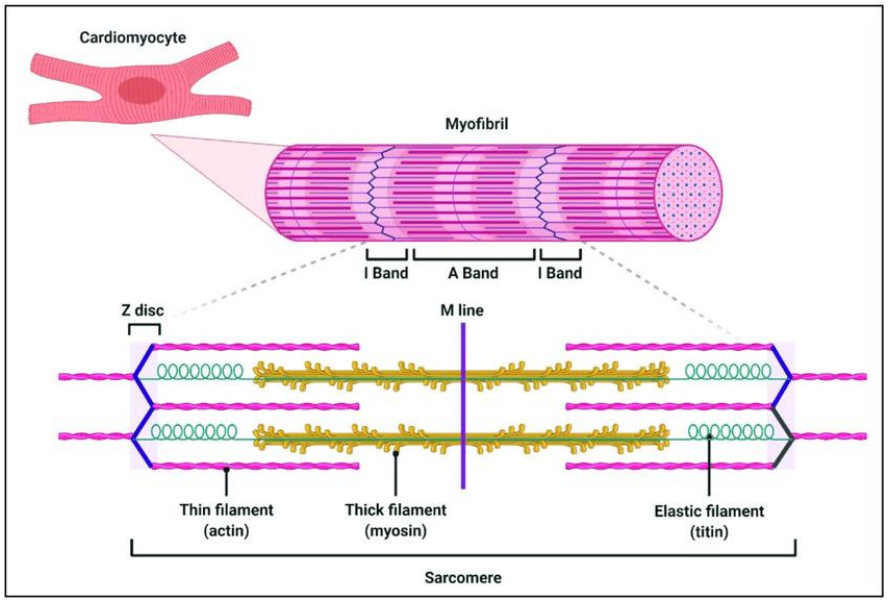

Figure 1.3.1 - Schematic of sarcomere structure (Santiago et al., 2021).

The thin filament is composed of a double-stranded helix of filamentous actin (F-actin), along with two tropomyosin (Tm) strands and three troponin (Tn) subunits, namely TnT, TnI, and TnC. These components collectively create the calcium (Ca2+) regulatory complex of the thin filament. The Tm strands are positioned within the two grooves of F-actin, offering stability, flexibility, and cooperativity to the thin filament (Crocini & Gotthardt, 2021).

The thick filament notably consists of motor proteins called myosin, that convert chemical energy in the form of Adenosine 5'-triphosphate (ATP) to mechanical energy, producing movement and force allowing muscle contraction (Cooper, 2000).

Myosin II is the type of myosin present in muscle, consisting of two identical coiled-coiled myosin heavy chains (MyHC), two regulatory light chains (RLC), and two essential light chains (ELC). Each heavy chain possesses a globular head region, with an actin-binding site and an ATP-binding site, and a long α-helical tail. Heavy meromyosin (HMM) constitutes the globular head region located within the thick filament of muscle fibers. It comprises two distinct subunits known as S1 (Subfragment 1) and S2 (Subfragment 2) (Figure 1.3.2) (Barrick & Greenberg, 2021).

ELC and RLC are important for myosin conformation and plays an essential role in altering the interaction between actin and myosin, so when mutations or changes occur on these structures, it can lead to cardiac-related diseases (Barrick & Greenberg, 2021; Muthu et al., 2011).

The transition between the 'OFF' and 'ON' states of the myosin heads are under the modulation of the phosphorylation state of the RLC. The central function of the RLC segment within myosin involves overseeing the availability of myosin heads for interaction with actin. The phosphorylation process of RLC plays a pivotal role in regulating cardiac contractility by impacting the interaction between the RLC segment of myosin heads and the thick filament (Kampourakis et al., 2015). There is existing data indicating that modifications of ELC can potentially influence the cross-bridging between myosin and actin, myosin ATPase activity, and calcium utilization. As a result, these modifications may serve as a molecular regulator, influencing the generation of muscle force (Scheid et al., 2016).

Cardiac myosin binding protein-C (cMyBP-C) is a sarcomeric protein closely associated with thick filaments and found in cardiomyocytes in the C-zone of the A-band. MyBP-C was demonstrated to tethered to the thick filament primarily through its C-terminus, where it forms connections with the light meromyosin and titin. Furthermore, the N-terminal region of MyBP-C interacts with myosin by binding to the RLC and to the sub-fragment 2 (S2) region of the myosin tail. It is theorized that MyBPC primarily regulates contraction through its N-terminus, playing a pivotal role in modulating cardiac contractility by engaging in transient interactions with both thick and thin filaments to regulate actomyosin interactions (Lee et al., 2015; Oakley et al., 2007).

The significance of cMyBP-C becomes evident when considering that mutations in the MYBPC3 gene, which encodes this sarcomeric protein, represent the most prevalent cause of hypertrophic cardiomyopathy (HCM) (McNamara et al., 2019). One study refers that when examining cardiomyocytes with hypertrophic cardiomyopathy mutations in MYBPC3, it becomes apparent that these mutations lead to the direct activation of myosin contraction by disturbing the relaxed states of myosin (Toepfer et al., 2019).

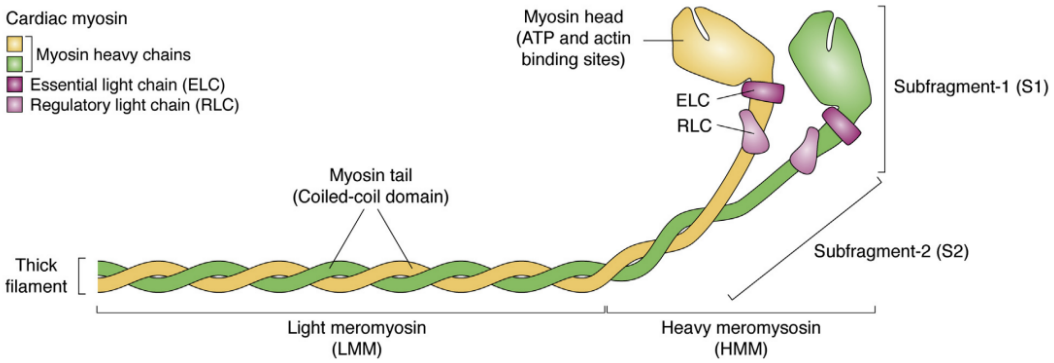

Figure 1.3.2 – Cardiac myosin structure. Yellow and green represent heavy chains, each bound to an essential light chain and a regulatory light chain. The subfragment-1 region corresponds to the myosin heads. Light meromyosin is the tail region and heavy meromyosin is the globular head region. The myosin tail (light meromyosin) assembles into the tick filament (Barrick & Greenberg, 2021).

The cross-bridges between the thick and thin filaments are a result of the binding between the globular heads of myosin to actin. The myosin heads also bind and hydrolyze ATP, which provides energy for the sliding between the filaments. In the absence of ATP, myosin is tightly bound to actin. When ATP binds to myosin, dissociates the myosin-actin complex and the consequent hydrolysis of ATP provokes a conformational change in myosin. Adenosine diphosphate (ADP) and inorganic phosphate (Pi) are the products from hydrolysis and remain bound to the myosin head. When the myosin head binds again to the actin filament, the ADP and Pi are released, making the myosin head return to the initial conformation. This action promotes the sliding of the actin filament in the direction of the M line of the sarcomere (Figure 1.3.3) (Cooper, 2000).

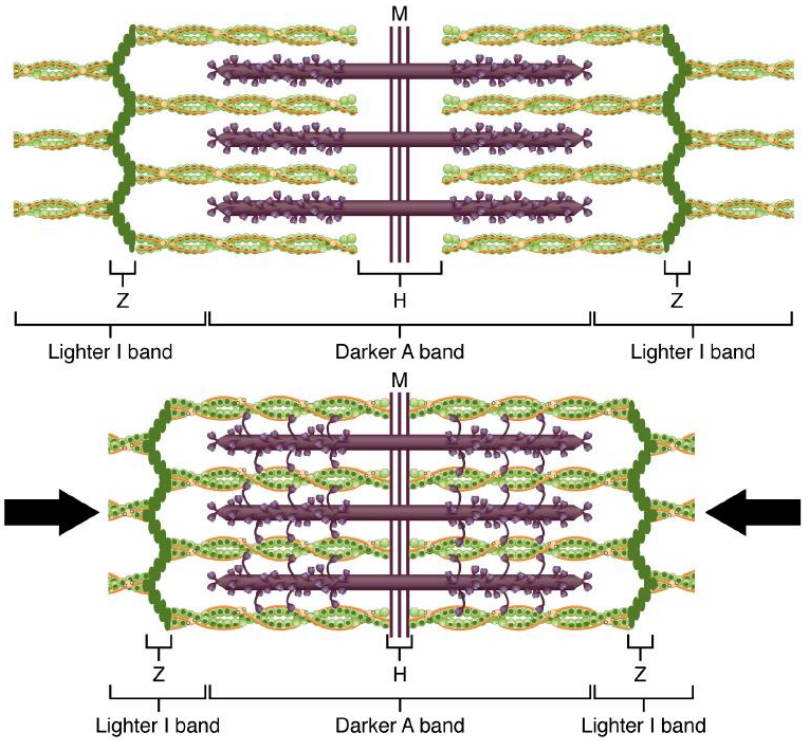

Figure 1.3.3 – When the contraction of the sarcomere occurs, the Z lines move closer, resulting in a reduction of the I band's size (Betts et al, 2022).

1.4 Muscle Contraction

The process of muscle contraction is powered by the interaction between two key proteins, myosin and actin, and energized through the hydrolysis of ATP (Irving, 2012).

Contraction in muscle occurs when the myosin S1 heads from the thick filament attach to actin molecules in the thin filament and generate force. This force leads to the sliding of the thin filament over the thick filament, resulting in the shortening of the sarcomere and the development of force (Gordon et al., 2001).

Muscle activation is initiated by the liberation of Ca2+ from calcium reservoirs within the membranous sarcoplasmic reticulum encompassing muscle myofibrils. This release is prompted by neural signals originating in the brain and transmitted through motor nerves to the fiber membrane, known as the sarcolemma, which undergoes depolarization, making it possible for these signals to reach all myofibrils. Once Ca2+ is discharged into the myofibrils, it associates with troponin-C (TnC) situated on the actin filaments. This interaction prompts a structural alteration in troponin, leading to a movement of the tropomyosin strands it is connected to, along the surface of the actin filament. This alteration in tropomyosin position, facilitated by calcium binding, modifies the binding site on sub-domain 1 of actin to which the myosin heads must adhere. Consequently, the heads attach to actin, enabling the contractile cycle to commence (Squire, 2019).

The regulation of muscle contraction by Ca2+ primarily occurs through alterations in the thin filament, although modulation can also occur through myosin. Regulatory proteins tropomyosin (Tm) and troponin (Tn) are attached to actin (A). Tm, a long and flexible molecule, binds to seven actin monomers along the thin filament helix, overlapping with adjacent Tm molecules. Tn attaches to two actin molecules when Ca2+ is absent, with its TnI subunit connecting to actin and its TnT subunit linking to Tm. When Ca2+ binds to the TnC subunit, it strengthens the interaction between TnC and TnI, causing TnI to disengage from its contacts with actin. When a myosin cross-bridge is firmly bound to actin, Tm becomes locally stabilized in a position that exposes myosin binding sites on nearby actin monomers. Therefore, structural data suggests that the activation of the thin filament is achieved by the movement of Tm across the actin surface, which is regulated by both Ca2+ binding to TnC and the initial binding of cross-bridges to actin, enabling additional strong cross-bridge binding. In the presence of saturating Ca2+, Tm's position allows approximately 20% of the actin sites to be in the open state at any given time, while about 80% remain in the closed state (Gordon et al., 2001)

1.5 Myosin Conformations

Relaxed myosin can be found in two different conformations: disordered-relaxed state (DRX), where one of the two myosin heads is blocked because it is folded, resulting in only one myosin head available to hydrolyze ATP; and super-relaxed state (SRX) where both ATP-binding domains are incapable to bind actin since they are sterically inhibited with both heads folded. In the SRX, myosins do not participate in contraction, and in case of increased mechanical need, they provide reserve heads that can be activated (Figure 1.5.1). In this state, since the myosin heads are bound to each other along the thick filament, SRX has a highly inhibited rate of ATP turnover (Crocini & Gotthardt, 2021; McNamara et al., 2015; Toepfer et al., 2020).

The duration of SRX activity within cardiac muscle is notably briefer compared to skeletal muscle, involving the hydrolysis of a single ATP roughly every 145 seconds per myosin head (McNamara et al., 2015).

The SRX and DRX are supposed to be in equilibrium, where the dysregulation of the SRX in either inherited or acquired cardiac conditions, can influence the contractile function of the cardiomyocyte. In HCM, myosin mutations can promote a shift in equilibrium that can result in more heads being available for interaction with actin which can explain the hypercontractility seen clinically (Anderson et al., 2018; Schmid et al., 2021).

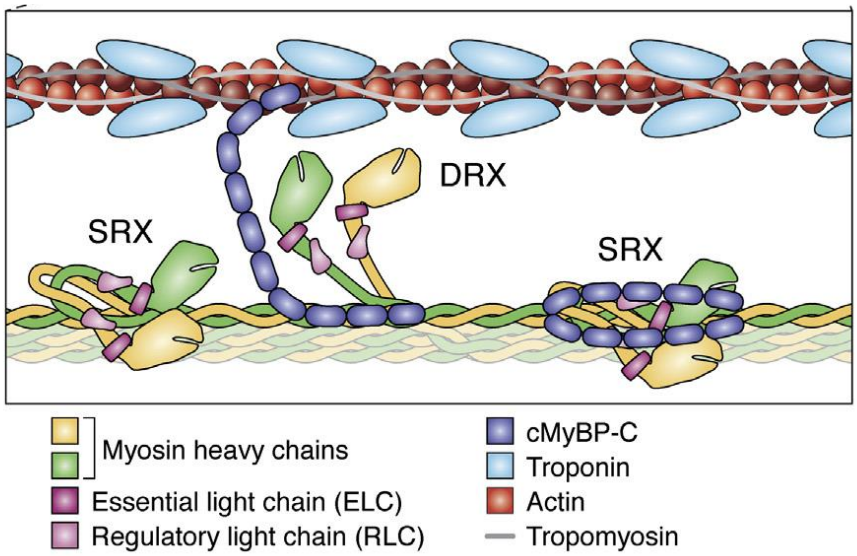

Figure 1.5.1 – Illustration of the super-relaxed state and the disordered-relaxed state. In the super-relaxed state, the myosin heads are bound to the thick filament, while in the disordered-relaxed state they are free (Barrick & Greenberg, 2021).

Multiple intramolecular connections have been detected between the two heads of a single myosin molecule, known as the "interacting-heads motif" (IHM). Myosin filaments with this structure are present in the SRX state, where the myosin motors interact with each other and fold back against the S2 fragment, in which the usage of ATP is minimised. The SRX state is kept closed by the IHM (Day et al., 2022).

These interactions extend to involve both heads and encompass the ELC and RLC. In this arrangement, the converter domain of the unengaged head interacts with the actin-binding domain of the hindered head, resulting in the deactivation of both heads. This mechanism not only inhibits the obstructed head's ability to bind to actin but also restricts the ATPase activity of the unoccupied head. The reduction in ATP turnover observed in the SRX state is believed to result from these intramolecular and intermolecular interactions, along with the attachment of myosin heads to the thick filament (McNamara et al., 2015).

IHM interactions are crucial for the regulation and sustenance of sarcomeric contractility, a particularly vital feature for adapting cardiac output in the heart. The IHM regulatory complex consists of the ELC, which contains a Ca2+ binding site, and the RLC. In human myocardium, the RLC has a single serine residue that can be phosphorylated by the cardiac myosin light chain kinase, adding another layer of regulation to this complex system (Schmid et al., 2021).

1.6 Hypertrophic Cardiomyopathy (HCM)

HCM is a genetic cardiac disorder with an estimated prevalence of 1 in 500 people, characterized by LV hypertrophy that can result in hypercontractility, left ventricular outflow tract (LVOT) obstruction, increased energy consumption by the heart, arrhythmic sudden death and heart failure (Maron et al., 2022; Toepfer et al., 2020). It ranks among the more frequent inherited cardiac conditions and stands as the primary cause of sudden cardiac death in young individuals who seem to be healthy (McNamara et al., 2016). The thickened septum causes obstruction to the blood flow since it affects the load enforced on the left ventricle and its contractility (Figure 1.6.1) (Nishimura et al., 2017).

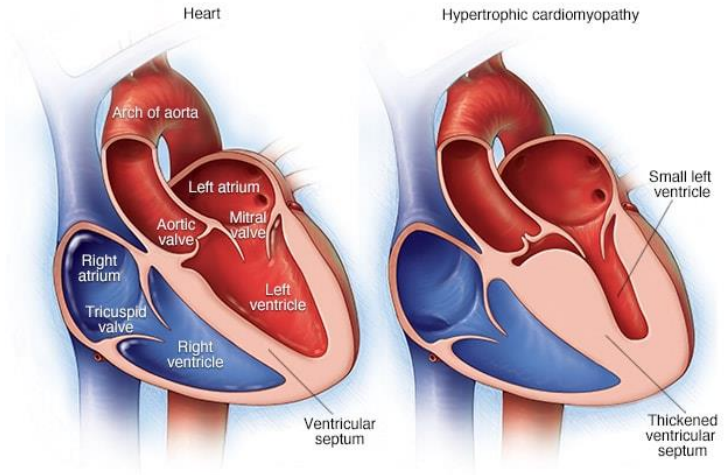

Figure 1.6.1 - Illustration of the differences between a healthy hearth and a hearth with hypertrophic cardiomyopathy (Mayo Clinic, 2022).

Myectomy is a surgery that removes part of the cardiac tissue that is obstructing the valves and it is done when patients present LVOT obstruction. This procedure is performed to lessen the symptoms but does not cure the disease (Nishimura et al., 2017).

The individuals diagnosed with HCM who lack any apparent family history of the condition and do not exhibit any identifiable genetic cause (referred to as nonfamilial HCM) exhibit distinct clinical characteristics that imply an alternative underlying pathogenesis. This subset constitutes 40% of all HCM cases and demonstrates a more favorable clinical trajectory, characterized by delayed onset of symptoms and improved event-free survival from major cardiovascular events (Ingles et al., 2017).

Around 50% of patients with HCM carry a sarcomere gene mutation (sarcomere mutation-positive, SMP), while the other half of the patients are sarcomere mutation-negative (SMN) where the genetic background is still unknown (Mosqueira et al., 2019). In SMP, the release of excessive myosin heads from the SRX state is promoted, increasing the overall ATP consumption (Ma et al., 2021).The major mutations in SMP are in genes encoding proteins like MYH7 and MYBPC3, encoding β-myosin heavy chain and myosin binding protein C, respectively. The majority of HCM variants in MYBPC3 encode truncations that promote a shift in the amount of myosins in DRX, increasing myosin contractility (Toepfer et al., 2020).

One study showed that 30% to 60% of individuals diagnosed with HCM do not exhibit germline mutations when screened for mutations in sarcomere genes. Additionally, patients with SMN were found to be markedly less likely to have a family history of HCM, tend to develop symptoms later in life, and are more likely to be obese compared to patients with HCM who do have sarcomere gene mutations (De Feria et al., 2021).

1.7 Mavacamten

In patients with HCM, pharmacological interventions often become necessary to manage symptoms such as limiting heart failure and angina, LVOT obstruction, and arrhythmias (Spoladore et al., 2012).

Molecular features of HCM include excess myosin actin cross-bridge formation and dysregulation of the SRX. Mavacamten (MYK-461) is small-molecule allosteric and reversible inhibitor of cardiac myosin ATPase that normalizes the hypercontractility of the sarcomere by binding directly to myosin, which inhibits excessive myosin actin cross-bridge formation. It is an investigational drug that may interrupt the development of hypertrophy and clinical complications seen in HCM (Anderson et al., 2018; Keam, 2022).

Several studies reported that MYK-461 reduces cardiac muscle contractility by shifting the balance more towards the SRX state, to restore the myosin DRX-SRX equilibrium (Figure 1.7.1) (Anderson et al., 2018; Gollapudi et al., 2021; Rohde et al., 2018; Toepfer et al., 2020).

Mavacamten functions by reducing the number of myosin heads capable of entering the power-generating state on actin, thereby lowering the likelihood of cross-bridge formation in HCM. This alteration in the overall myosin population shifts it towards the energy-conserving 'off state.' Therefore, as demonstrated in preclinical studies, mavacamten reduces the overall consumption of ATP in the sarcomere and promotes relaxation. This collection of direct and advantageous effects on diastolic, systolic, and energy-saving aspects leads to an enlargement of the ventricular chamber size and a decrease in the velocity of myocardial contraction, which establishes a greater intraventricular environment to mitigate LVOT obstruction (Edelberg et al., 2022).

Mavacamten emerges as a valuable pharmaceutical option for HCM. Its favorable impacts encompass a reduction in LVOT gradient, an increase of exercise capacity, and a decrease in biomarker levels, signifying diminished wall stress and ischemic injury. Additionally, observed improvements in clinical condition and overall quality of life align with these hemodynamic shifts. Notably, Mavacamten stands as a pioneering drug in its class, directly addressing the fundamental molecular mechanisms driving cardiomyocyte hypercontractility in HCM (Pysz et al., 2021).

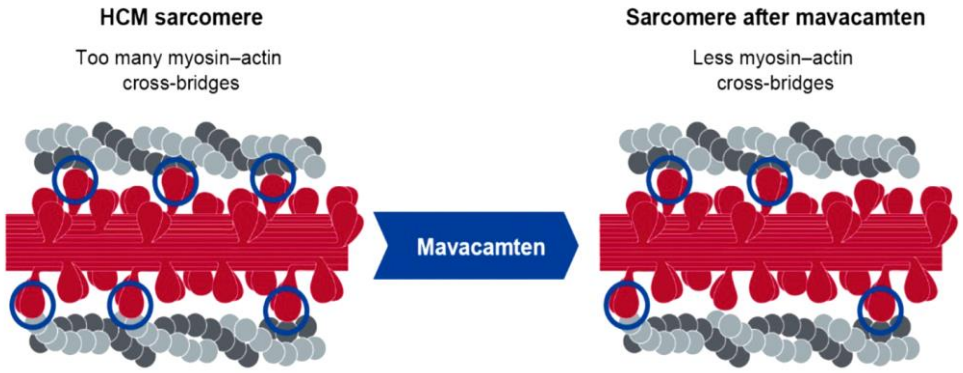

Figure 1.7.1 – Effect of Mavacamten on myosin (Pysz et al., 2021)

2. Hypothesis And Objectives

HCM is one of the leading genetic causes of cardiac failure and death. Its underlying mechanisms remain unclear but have been linked to a dysfunction of the most abundant protein in the heart, myosin.

In the present dissertation, myosin relaxed conformation and ATP consumption were tested in myectomies from healthy donors and from HCM patients. The workflow was dissecting cardiac strips, mount them in specific flow chambers and run a method called 2'-(or-3')-O-(N-Methylanthraniloyl)-Adenosine-5'-Triphosphate, trisodium Salt (MANT-ATP) chase experiment consisting of following the decay of fluorescent ATP over time in the cardiac strips. From these experiments, the result was a precise definition of myosin relaxed states and ATP consumption.

The samples used in this study were from HCM patients that have sarcomeric and non-sarcomeric mutations. Considering this, the aim of this dissertation is to:

(1) analyse if the Super Relaxed State – Disordered Relaxed State (SRX-DRX) equilibrium is altered, thereby leading to an over-consumption of ATP, in samples from Sarcomere Mutation Positive (SMP) and Sarcomere Mutation Negative (SMN) patients with HCM;

(2) investigate if the addition of Mavacamten (MYK-461) restores de SRX-DRX equilibrium, preventing an over-consumption of ATP;

(3) compare the SRX-DRX equilibrium between the HCM patients and the healthy donors.

3. Material And Methods

The experiments conducted throughout this dissertation were carried out in a "semi-blinded" manner. In this approach, information pertaining to the patients, such as the type of mutation and the severity of cardiac symptoms, remained unknown. However, the distinction between samples obtained from donors and those from patients was known. Complete details were disclosed only at the end of the study when all the data was analyzed. This methodology was employed to prevent any inadvertent biases from influencing the outcomes.

3.1 Cardiac Tissue

In the present study, fourteen left ventricle samples from patients with HCM and one donor sample were used (Table 3.1.1). Seven were from SMN patients and the remaining samples were from SMP patients: two with a MYH7 mutation and five with a MYBPC3 mutation.

All the samples were from myectomy surgeries that removed part of the septum of the left ventricle to relieve the valve obstruction.

The biobank at the VU University Medical Center in Amsterdam was responsible for flash-freezing, cryopreservation and storage of the samples in the -80 °C freezers. All these procedures were ethically approved in Amsterdam (Appendix 1). Once stored, the samples were shipped to the University of Copenhagen (Denmark) for further analysis.

Table 3.1.1 - Available information on the patients, their mutation, gender, age, Body Mass Index (BMI) and Left Ventricule (LV) ejection fraction.

Sample Identification	Genotype	Age at Surgery	Gender	Body Mass Index (BMI)	Left Ventricule Ejection Fraction (%)
233	**SMN**	37	M	30.41	Not available
244	**SMN**	75	M	27.26	60
247	**SMN**	65	F	24.20	Not available
257	**SMN**	70	F	33.80	65
259	**SMN**	51	F	25.3	70
262	**SMN**	59	M	25.3	65
263	**SMN**	58	M	30.10	70
236	**MYH7**	29	M	22.34	70
239	**MYBPC3**	69	F	25.96	60
246	**MYBPC3**	57	F	25.69	67
251	**MYBPC3**	63	M	31.22	70
252	**MYH7**	25	M	20.67	66
253	**MYBPC3**	54	F	28.70	Not available
256	**MYBPC3**	48	M	21.28	70
1708	**Donor**	Not available	Not available	Not available	Not available

3.2 Storage Of The Tissue

The cardiac samples were stored in the freezer at -80ºC. Only small strips of cardiac tissue were required for the project in question, therefore, to preserve the original sample as much as possible, it was necessary to cut one small portion from the original cardiac biopsy. The cutting was done in the cryo-chamber, where the samples could remain at low temperatures.

The biopsy was stored again in the -80ºC freezer, while the samples that were cut were kept in an eppendorf with a membrane-permeabilizing solution composed by 50/50 v/v glycerol and relaxing buffer (4 mM Mg-ATP, 1 mM free Mg2+, 20 mM imidazole, 7 mM EGTA, 14.5 mM creatine phosphate, KCl to adjust the ionic strength to 180 mM and pH to 7.0) at -20ºC for 24 hours (Appendix 2). After that time, the samples had to stay in the fridge at 4ºC for 18-24 hours, to allow a proper skinning process, and then be stored at -20ºC for up to 12 weeks. At this point, the samples were ready for dissection.

The glycerol induces notable changes in the morphology of T-tubules/sarcolemma by creating an osmotic shock that has the capacity to the disrupt the T-tubule network into multiple vacuoles. These vacuoles may either retain connections through conventional T-tubules or become isolated from each other (Al-Qusairi et al., 2011).

By employing EGTA on the relaxing buffer, which effectively chelates Ca2+, it is possible to investigate the structure of the thick filament without the complicating influence of thin filament activation (McNamara et al., 2017).

3.3 Sample Preparation

Before dissecting, it was necessary to prepare a microscope slide (Epredia) where the strips would be placed. Using the Zeiss Stemi 305 EDU microscope, a half-split copper grid (SPI supplies) designed for electron microscopy (Appendix 3), was glued to the microscope slide so it could be possible to hold the dissected strips in the middle of the copper grid (Figure 3.3.1).

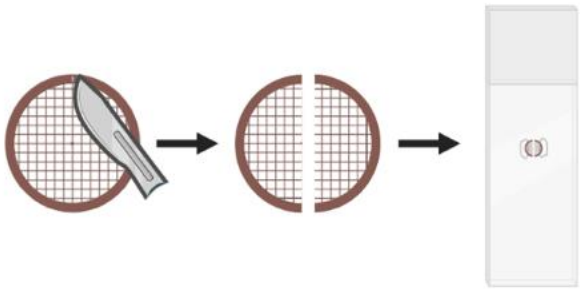

Figure 3.3.1 – Illustration of the process of cutting grids for the MANT-ATP chase experiment (Created with Biorender).

To dissect the cardiac strips, the first step was to take the sample out of the -20ºC freezer and put it on the Petri dish with relaxing buffer. The purpose of the relaxing solution was to relax the muscles, which in turn helps prevent the cardiac muscle from tearing apart during dissection. This makes the dissection process easier and more manageable.

Using the Zeiss Stemi 305 EDU microscope, with a syringe needle and a scalpel, the goal was to dissect thin strips from the cardiac sample and then hold them with the gramps from the grid that was placed in the slide. Relaxing buffer was always added to the microscope slide so the dissected strips that were mounted onto the grids did not dry out.

The last thing to do before the MANT-ATP chase experiment was to create a flow chamber by adding double-sided tape on both sides of the grid and a coverslip on top (Figure 3.3.2). This way, it was possible to ensure that the buffers passed through the dissected strips.

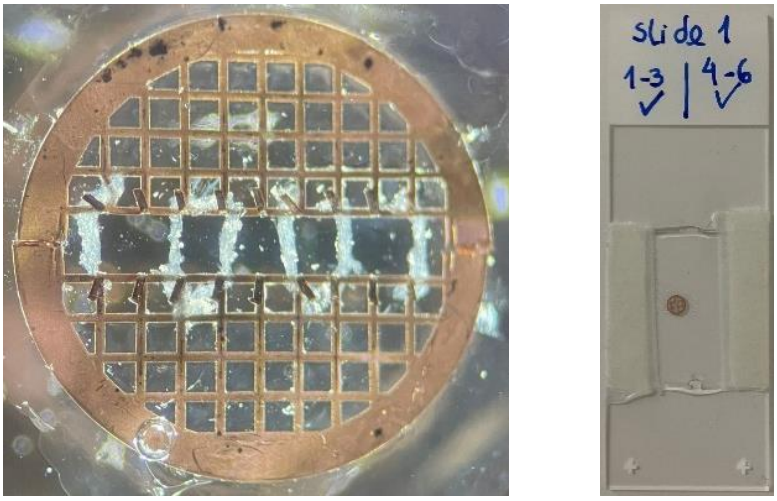

Figure 3.3.2 – Cardiac strips mounted onto the copper grids. The last picture is the slide fully prepared for the MANT-ATP chase experiment, with the flow chamber (Original photography).

3.4 The MANT-ATP Chase Experiment

The MANT-ATP chase experiment was performed to determine the distribution of SRX/DRX. This is a quantitative epi-fluorescence microscopy method, where the mant-nucleotides bound to myosin in order to measure the SRX-DRX equilibrium (Naber et al., 2011). MANT-ATP is an analog of ATP that significantly changes its emission intensity when bound to myosin, with an increase in fluorescence emission. When the association between myosin and MANT-ATP is lost, there is a decrease in the fluorescence. The changes in fluorescence make it possible to measure the binding and dissociation of MANT-ATP (McNamara et al., 2015).

Three solutions are required to be prepared for the MANT-ATP experiment: Rigor buffer (to remove ATP and glycerol), 250 μM MANT-ATP buffer and 4 mM ATP chase buffer (Appendix 4). It is mandatory to keep them always on ice.

The MANT-ATP chase experiment was done with a fluorescence microscope placed in a dark room. There, the strips were first washed three times with 90 μL rigor buffer for 5 minutes. Then, 90 μL of the MANT-ATP solution was flushed for 5 minutes in a dark chamber.

After Mant-ATP incubation, the slide was placed onto the Zeiss Axio Observer Scope microscope with 10x zoom, and the "Zen blue edition" program was used. 90 μL ATP chase buffer, containing rigor buffer and ATP, was added and frames were acquired every 5 seconds, for 5 minutes with a 20 ms acquisition/ exposure time using a DAPI filter set with Axiocam 705, Colibri 5/7, HAL 100.

The fluorescence decays when the ATP is flushed, as the Mant-nucleotides are released from the strips and are replaced by ATP. The myosin molecules contain an ATP binding site which has much more affinity with ATP over MANT-ATP, resulting in a decay over time (Naber et al., 2011). The decline in light intensity can be identified and used for quantifying the content of SRX and DRX, thereby facilitating the assessment of the SRX/DRX distribution.

Samples from 15 patients were analyzed and 4 slides were done per patient: two with Mavacamten and two without Mavacamten. For every slide, 6 cardiac strips were dissected, which means that 24 cardiac strips were mounted for each sample. In total, for all the 15 samples, 360 cardiac strips were mounted. For the samples treated with MYK-461, the protocol used was the same as the one described before, with the only difference being the addition of 1 μM MYK-461 in the three solutions used in the MANT-ATP chase experiment (Appendix 2).

3.5 Quantification And Statistical Analysis

Using the ImageJ program, the fluorescence decay was measured in each strip. The mean background fluorescence intensity was subtracted from the average strip fluorescence intensity for each image taken.

The statistical analysis was performed with GraphPad Prism 9.0 software using a two-phase decay exponential function that measures the decay in fluorescence intensity (McNamara et al., 2017):

$$\mathrm{I}{=}1-\mathrm{P}_1\left(1-exp\left(\frac{-\mathrm{t}}{\mathrm{T}_1}\right)\right)-\mathrm{P}_2\left(1-exp\left(\frac{-\mathrm{t}}{\mathrm{T}_2}\right)\right)$$

In this function, (I) is fluorescence intensity, P1 and P2 are the initial proportions of fluorescence for each state (DRX and SRX), (t) is the time in the ATP chase and T1 and T2 are the time constants for the lifetime of these states. P1 and T1 represent the initial rapid decay in fluorescence intensity, which correlates with myosin in the DRX state and the release of non-specifically bound MANT-ATP. P2 and T2 are representative of the subsequent slow decrease in fluorescence intensity due to myosin in the SRX state (McNamara et al., 2016). The resulting data are the percentage of myosin in the SRX and in the DRX on each cardiac strip.

Statistical testes were run considering two factors: group (donors vs SMP vs SMN) and treatment (with MYK-461 vs without MYK-461). The results obtained from the two-phased decay process were averaged for each specific group. To analyze the data, a two-way ANOVA was conducted using GraphPad Prism 9.0, followed by a Tukey post hoc analysis. Statistical significance was considered significant at a threshold of $p<0.05$, to test whether the cardiac muscle had different DRX/SRX distribution with and without mavacamten.

4. Results

4.1 Analyse If The SRX-DRX Equilibrium Is Altered

To test if the SRX-DRX equilibrium was altered, an Ordinary One-Way ANOVA was performed (Figure 4.1.1 and 4.1.2). Statistical significance was considered significant at a threshold of $p<0.05$.

The p-value obtained from the analyse of P1 was p = 0,0091, and the p-value from the analyses of P2 was p = 0,0078. These p-values signify that the difference between the samples are statistically significant.

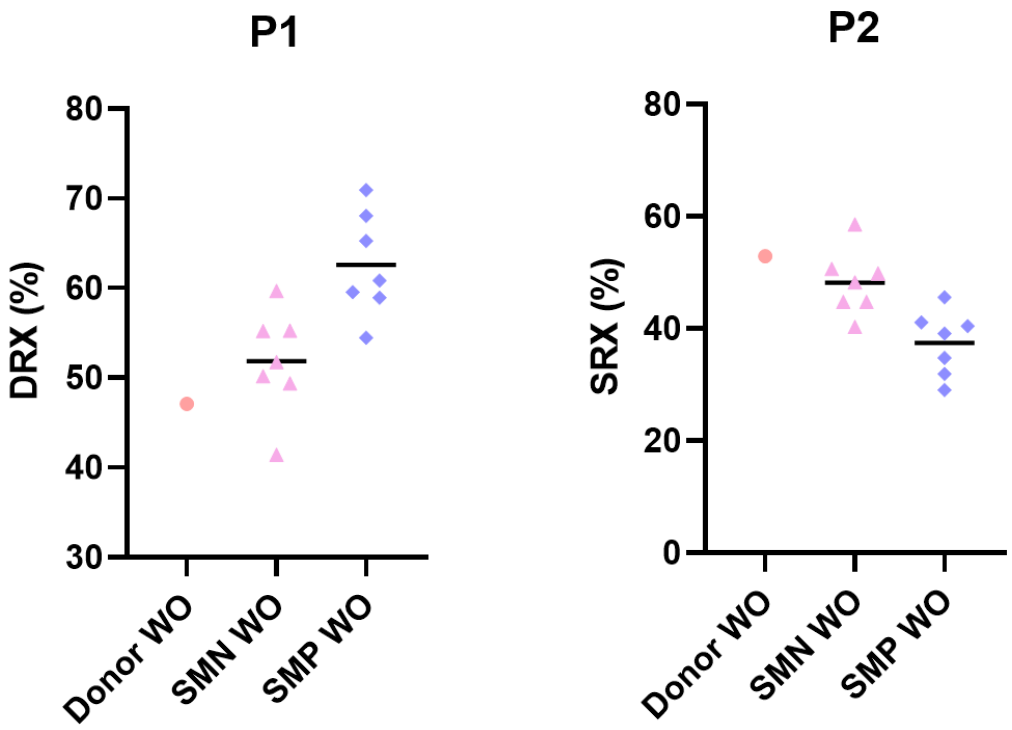

Figure 4.1.1 and 4.1.2 - Plots showing the mean of P1 (index of DRX) and P2 (index for SRX) from each sample without mavacamten, as larger colored figures.

4.2 Investigate If The Addition Of Mavacamten (MYK-461) Restores The SRX-DRX Equilibrium

The following results were obtained from the statistical tests between group (donors vs SMP vs SMN) and treatment (with MYK-461 vs without MYK-461) (Figure 4.2.1 and 4.2.2, Table 4.2.1, Table 4.2.2, Figure 4.2.3 and Figure 4.2.4, Table 4.2.3, Table 4.2.4):

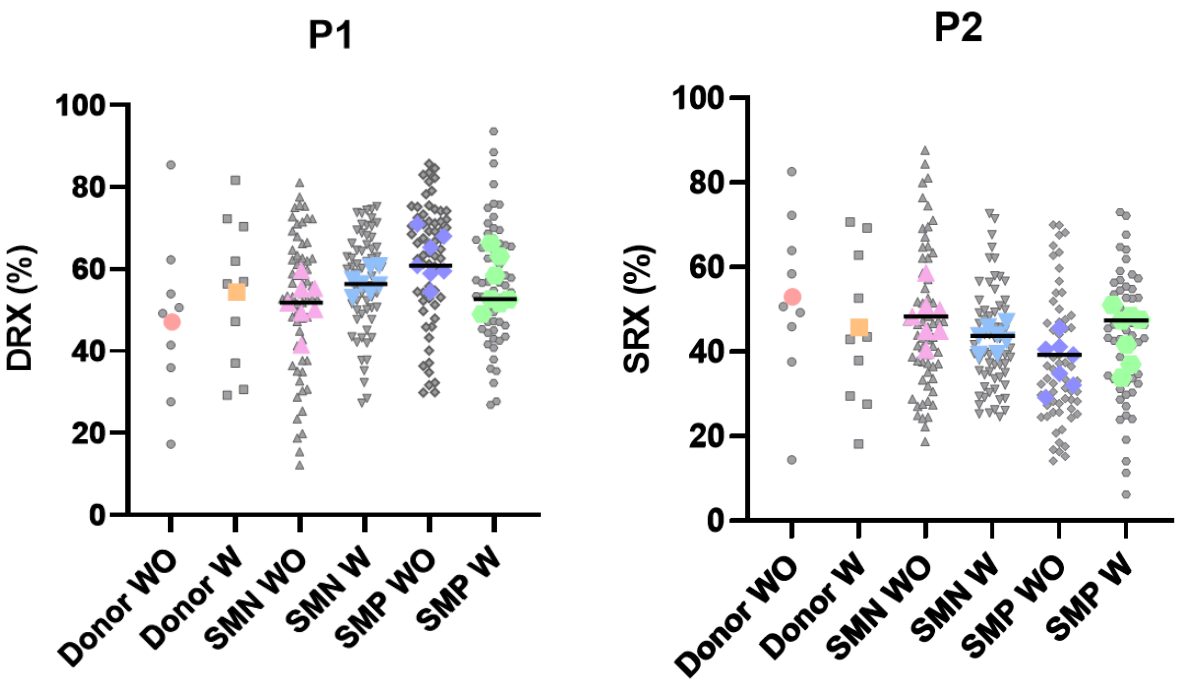

Figure 4.2.1 and 4.2.2 - Super plots showing all single fibers used in the Mant-ATP chase experiment presented as small light gray figures and the mean of each sample as larger colored figures. Plot of P1 (index of DRX), where the initial rapid decay correspondes to DRX. Plot of P2 (index of SRX), where the slow decay correspondes to SRX.

Table 4.2.1 – P1 statistical results from the 2way ANOVA

Source of Variation P1	% of total variation	P value	Significant?
Mavacamten	1,385	0,4625	No
Patient	19,78	0,0321	Yes

Table 4.2.2 – P2 statistical results from the 2way ANOVA

Source of Variation P2	% of total variation	P value	Significant?
Mavacamten	1,177	0,4929	No
Patient	20,43	0,0271	Yes

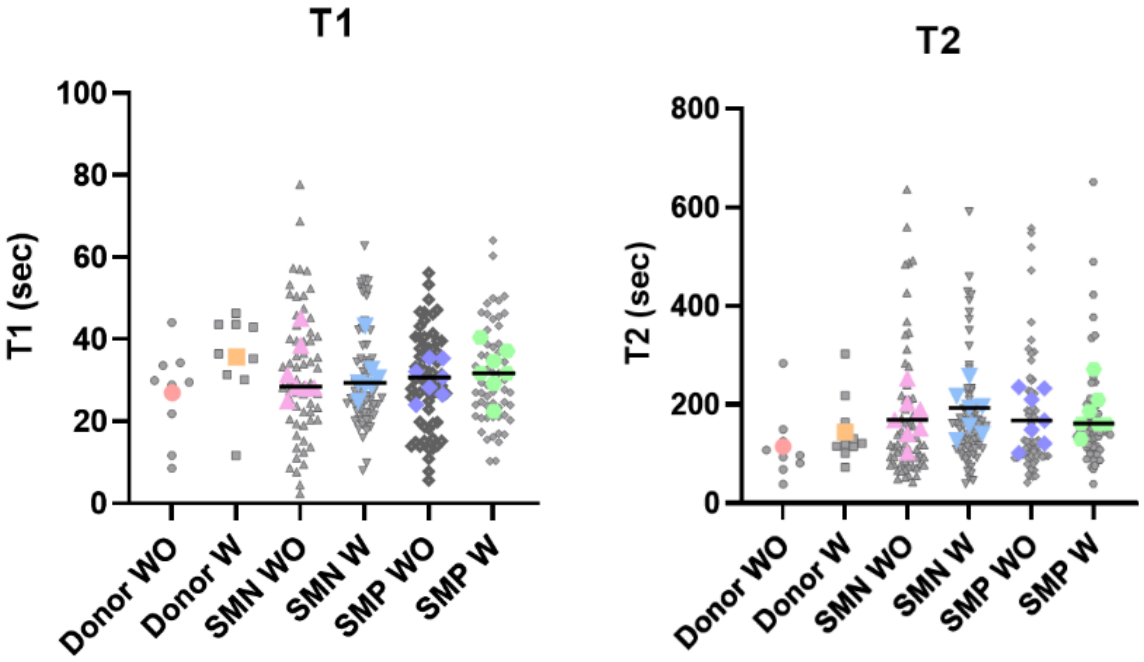

Figure 4.2.3 and 4.2.4 – Super plots showing all single fibers used in the Mant-ATP chase experiment presented as small light gray figures and the mean of each sample as larger colored figures. Plot of T1 (index of DRX ATP turnover time) and plot of T2 (index of SRX ATP turnover time).

Table 4.2.3 – T1 statistical results from the 2way ANOVA

Source of Variation T1	% of total variation	P value	Significant?
Mavacamten	1,545	0,5293	No
Patient	7,147	0,4036	No

Table 4.2.4 – T2 statistical results from the 2way ANOVA

Source of Variation T2	% of total variation	P value	Significant?
Mavacamten	4,292	0,3042	No
Patient	0,04622	0,9941	No

P1 and P2 showed a significant difference (Table 4.2.1 and Table 4.2.2) in the DRX and SRX percentage between the SMP, SMN and donors samples, but not between the samples with and without mavacamten (Figure 4.2.1 and 4.2.2).

The two time constants, T1 and T2, at which a myosin head hydrolyzes ATP in the DRX and SRX state, respectively, did not show any significant difference between donors, SMP and SMN patients (Table 4.2.3 and Table 4.2.4), with or without mavacamten (Figure 4.2.3 and 4.2.4).

4.3 Compare The SRX-DRX Equilibrium Between The HCM Patients And The Healthy Donors

A two-phased exponential decay analysis was done for every cardiac strip and P1 (index of DRX), P2 (index for SRX), T1 (index of DRX ATP turnover time), and T2 (index of SRX ATP turnover time) were calculated to get the final percentage of DRX and SRX.

Table 4.3.1 summarizes the mean ±S.E.M. for P1, P2, T1, and T2 for all the strips that were included.

Table 4.3.1 - Summarizes the mean ±S.E.M. for P1 (index of DRX), P2 (index of SRX), T1 (index of DRX ATP turnover time), and T2 (index of SRX ATP turnover time) for all the strips that were included.

SAMPLE		P1 (%)	P2 (%)	T1 (s)	T2 (s)
Donor	**Donor 1708 WO**	47.09778	52.902	26.94367	115.4444
	Donor 1708 W	54.377	45.623	35.673	145.313
MYBPC3	**HCM 239 WO**	59.54778	40.452	28.28556	211.2444
	HCM 239 W	66.27727	33.723	22.48364	161.1827
	HCM 246 WO	54.46111	45.539	24.02456	102.6644
	HCM 246 W	49.01111	50.989	40.45889	272.4556
	HCM 251 WO	68.07571	31.924	30.68429	168.5171
	HCM 251 W	63.09	36.910	34.66875	210.325
	HCM 253 WO	62.467	37.533	33.27	447.116
	HCM 253 W	52.514	47.486	31.713	130.361
	HCM 256 WO	58.92182	41.078	35.35182	233.6245
	HCM 256 W	52.70286	47.297	37.09857	160.6229
MYH7	**HCM 236 WO**	63.3525	36.648	31.71413	211.6588
	HCM 236 W	58.49556	41.504	29.22556	187.3311
	HCM 252 WO	60.87417	39.126	26.54167	121.4242
	HCM 252 W	51.665	48.335	31.74625	162.5063
SMN	**HCM 233 WO**	41.44444	58.556	25.07222	104.4167
	HCM 233 W	53.056	46.944	32.651	217.93
	HCM 244 WO	55.25	44.750	28.20356	152.0411
	HCM 244 W	56.0975	43.903	30.56275	193.4463
	HCM 247 WO	59.70833	40.292	38.555	203.69
	HCM 247 W	60.76875	39.231	29.4075	197.3275
	HCM 257 WO	55.2175	44.783	28.0475	169.5613
	HCM 257 W	57.43167	42.568	24.75175	127.5608

	HCM 259 WO	51.76667	48.233	31.37467	191.0967
	HCM 259 W	54.28	45.720	43.195	258.58
	HCM 262 WO	49.39625	50.604	28.48325	141.6225
	HCM 262 W	56.391	43.609	28.734	157.534
	HCM 263 WO	50.16714	49.833	45.16014	253.96
	HCM 263 W	60.661	39.339	28.63	141.98

According to Table 4.3.2, SMP patients tend to have a higher P1 compared to donors or patients with SMN mutations. Treatment with MYK-461 tended to lower P1 and increase P2 on SMP patients in contrast to donors and patients with SMN mutations. T2 appears to exhibit increased levels in all the samples treated with MYK-461, in contrast to those without treatment.

Table 4.3.2 - The average P1 (index of DRX), P2 (index of SRX), T1 (index of DRX ATP turnover time), and T2 (index of SRX ATP turnover time) from the results in table 4.3.1

Sample Mean	**P1**	**P2**	**T1**	**T2**
DONOR WO	47,09778	52,902	26,94367	115,4444
DONOR W	54,377	45,623	35,673	145,313
SMP WO	62.58362	37.416	30.34748	174.7714
SMP W	56.25083	43.749	32.48495	183.5406
SMN WO	51.85005	48.150	32.12805	173.7697
SMN W	56.95513	43.045	31.13314	184.9084

4.4 Other Results

The MANT-ATP chase experiment was used to measure the DRX and SRX states in each cardiac strip. As shown in the figure 4.4.1, the fluorescence decay is divided into a fast phase in the first few seconds, which is represented by the fast ATP turnover rate of DRX, and a slow phase which comes from the slow ATP turnover rate of SRX.

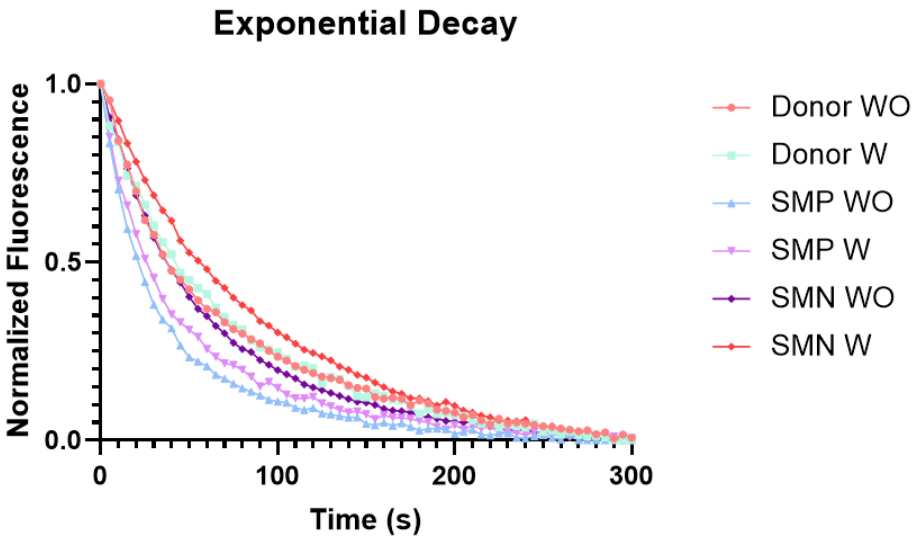

Figure 4.4.1 - Mant-ATP fluorescence decay caused by flushing with ATP. Data are fit by a double exponential decay to assess the DRX-SRX ratio.

In Figure 4.4.1 it can be observed that SMP samples show a much more rapid decay in contrast to donors and to SMN.

5. Discussion

In the present study, the ratio of Disordered-Relaxed State (DRX) and Super-Relaxed State (SRX) in myectomy samples from donors and from patients with Sarcomere Mutation Positive (SMP) and Sarcomere Mutation Negative (SMN) mutations, with and without Mavacamten (MYK-461) was studied.

The first goal of this thesis was to analyse if the SRX-DRX equilibrium was altered, thereby leading to an over-consumption of ATP, in samples from SMP and SMN patients with HCM. When comparing the HCM samples with the donor sample, by interpreting the statistical results of the P1 analysis, it is possible to deduce that there is a significant difference in the percentage of DRX, between the SMP, SMN and donor samples. These results were seen before, in a study by McNamara et al. (2017), where unlike donors, only samples with the MYBPC3 mutation (SMP) showed a decrease in SRX. These specific changes in the DRX-SRX equilibrium were not observed in samples with SMN.

The second goal was to investigate if the addition of MYK-461 restores de SRX-DRX equilibrium, preventing an over-consumption of ATP. The current research delved into assessing the impact of MYK-461 on HCM by examining samples from myectomy procedures obtained from both donors and patients with SMP and SMN mutations. The findings indicated that there was no statistically significant variance in the SRX-DRX ratio across all the groups, regardless of whether they were treated with MYK-461 or not. However, according to the figures from the results section, SMP samples with MYK-461 show a reduction in the percentage of DRX when compared to the SMP samples without MYK-461. MYK-461 tended to lower P1 and increase P2 for SMP patients in contrast to SMN patients and donors. Although these differences are not statistically significant, it is possible to deduce that MYK-461 causes an effect in the SMP samples, contrasting to SMN patients and donors. This was seen previously, in a study by Toepfer et al., 2019, that revealed that in skinned human heart fibers with heterozygous MYBPC3 truncations associated with HCM, there was an elevated proportion of myosin in the DRX state compared to normal human heart fibers. Interestingly, when MYBPC3-mutant fibers were treated with MYK-461, this treatment led to the normalization of the DRX/SRX ratio. This was achieved by simultaneously decreasing the myosin proportion in the DRX state while increasing the proportion in the SRX state. Several other studies also reported that MYK-461 reduced cardiac muscle contractility by shifting the balance more towards the SRX state, to restore the myosin DRX-SRX equilibrium (Anderson et al., 2018; Gollapudi et al., 2021; Rohde et al., 2018; Toepfer et al., 2020).

The third and last goal was to compare the SRX-DRX equilibrium between the HCM patients and the healthy donors. By interpreting the statistical results of the P1 and P2 analysis, it is possible to deduce that there is a significant difference between the SMP, SMN and donor samples, which means there is a significant difference in the percentage of DRX between the different groups of patients. When comparing the mean of each sample, it appears that the percentage of myosin in the SRX state is higher in the donor sample as compared to the HCM patients. Also, upon comparing all the P1 values, it is noticeable that SMP patients tend to have a higher P1 (a higher percentage of DRX), compared to donors or patients with SMN mutations.

As observed in the exponential decay, SMP samples showed a much more rapid decay in contrast to donors and SMN samples. McNamara et al (2017) also demonstrated an initial phase of rapid decline, succeeded by a more gradual phase. The gradual phase is indicative of the existence of myosin in the SRX. The reduction in fluorescence intensity follows a nearly identical pattern in both donors and SMN. Conversely, the same authors showed that the fluorescence

intensity diminishes notably quicker in the SMP samples, displaying a less pronounced gradual phase (McNamara, et al., 2017).

Dilated cardiomyopathy (DCM) and hypertrophic cardiomyopathy (HCM) stand out as the most prevalent subtypes of cardiomyopathies in patients. Both are hereditary and frequently lead to heart failure and arrhythmias but have distinct clinical presentations (Day et al., 2022). While HCM is marked by a reduction in left ventricular chamber size, along with fibrosis and myocyte disarray, individuals with hereditary dilated cardiomyopathy (DCM) exhibit decompensated cardiac hypertrophy, characterized by distended and thinly walled ventricles, accompanied by reduced contractility (Debold et al., 2007). These contrasting impacts on contractile function are partially attributed to the diverse effects of causal genetic variations on sarcomeric function, acting as the initiating factors for adverse cardiac remodeling (Day et al., 2022).

Given that mutations in myosin, are implicated in both HCM and DCM, investigating the impact of these mutations on myosin's force generation and motion offers a unique opportunity to comprehend how functional alterations give rise to such contrasting clinical manifestations (Debold et al., 2007). One compelling hypothesis posits that DCM mutations may stabilize the SRX state, thereby reducing the number of available myosin heads for generating contractile force, which could elucidate the observed hypocontractility. The study of Rasicci et al (2022), indicates that a solitary point mutation linked to DCM has a profound stabilizing effect on both the IHM conformation and SRX state. It is currently hypothesized that HCM mutations augment the force and power associated with myosin, whereas DCM mutations have the opposite effect.

Considering this, it could be intriguing to delve into a comparative study of DCM and HCM in relation to the SRX state. This is particularly relevant given the hypothesis that these two diseases have contrasting effects in this regard.

6. Conclusion

This dissertation had several limitations, including a restricted number of patients, leading to a limited dataset. The sample size of fifteen samples may not have provided sufficient statistical power to detect significant changes upon the application of MYK-461. Therefore, it is advisable to include a larger number of patients in future analyses to enhance the reliability of the findings. Additionally, the methods employed were highly time-consuming, making it impractical to collect a larger sample size due to the extensive time required for each individual sample's experimentation.

Furthermore, it is plausible that the discrepancy is associated with the methodology employed. If the study were to be replicated, one consideration could be increasing the mavacamten concentration to 10 uM as an adjustment. It is worth considering that cardiac strips possess greater thickness, which may hinder the proper binding of mavacamten to myosins. Another potential modification to explore would involve enhancing the permeabilization of the cardiac strips by substituting glycerol with Triton and performe an incubation for a duration of 1 hour. Using Triton, it may be worthwhile to investigate its potential to enhance permeability, facilitating improved diffusion of mavacamten into the cells.

Several studies reported that MYK-461 reduced cardiac muscle contractility by shifting the balance more towards the SRX state, to restore the myosin DRX-SRX equilibrium (Anderson et al., 2018; Gollapudi et al., 2021; Rohde et al., 2018; Toepfer et al., 2020). The expected decrease in DRX was not observed in the results obtained from this study.

It is important to highlight that the average was computed for each sample. This implies that MYK-461 could have demonstrated significant efficacy in certain cardiac strips while showing less effectiveness in others.

In summary, the next phase of the SMN research should involve the utilization of triton instead of glycerol to investigate if it is a diffusion-related issue. Additionally, the mavacamten concentration should be increased. To obtain more conclusive results, it is imperative to expand the study by including a larger sample size.

7. References

Al-Qusairi, L., & Laporte, J. (2011). T-tubule biogenesis and triad formation in skeletal muscle and implication in human diseases. *Skeletal Muscle* 1 (1), 26. https://doi.org/10.1186/2044-5040-1-26

Anderson, R. L., Trivedi, D. V., Sarkar, S. S., Henze, M., Ma, W., Gong, H., Rogers, C. S., Gorham, J. M., Wong, F. L., Morck, M. M., Seidman, J. G., Ruppel, K. M., Irving, T. C., Cooke, R., Green, E. M., & Spudich, J. A. (2018). Deciphering the super relaxed state of human β-cardiac myosin and the mode of action of mavacamten from myosin molecules to muscle fibers. *Proceedings of the National Academy of Sciences of the United States of America*, *115*(35), E8143–E8152. https://doi.org/10.1073/pnas.1809540115

Barrick, S. K., & Greenberg, M. J. (2021). Cardiac myosin contraction and mechanotransduction in health and disease. Journal of Biological Chemistry, 297(5), 1–16. https://doi.org/10.1016/j.jbc.2021.101297

Betts, J. G., Young, K. A., Wise, J. A., Johnson, E., Poe, B., Kruse, D. H., Korol, O., Johnson, J. E., Womble, M., & DeSaix, P. (2023). Anatomy and Physiology 2e. OpenStax. https://openstax.org/books/anatomy-and-physiology-2e/pages/1-introduction

Cooper, G. M. (2000). Actin, Myosin, and Cell Movement. *The Cell: A Molecular Approach* (2nd edition). Sunderland (MA): Sinauer Associates.

Crocini, C., & Gotthardt, M. (2021). Cardiac sarcomere mechanics in health and disease. *Biophys Rev*, *13*, 637–652. https://doi.org/10.1007/s12551-021-00840-7/Published

Day, S. M., Tardiff, J. C., & Michael Ostap, E. (2022). Myosin modulators: Emerging approaches for the treatment of cardiomyopathies and heart failure. *Journal of Clinical Investigation*, *132*(5), e148557. https://doi.org/10.1172/JCI148557

De Feria, A. E., Kott, A. E., & Becker, J. R. (2021). Sarcomere mutation negative hypertrophic cardiomyopathy is associated with ageing and obesity. *Open Heart*, *8*(1), e001560. https://doi.org/10.1136/openhrt-2020-001560

Debold, E. P., Schmitt, J. P., Patlak, J. B., Beck, S. E., Moore, J. R., Seidman, J. G., Seidman, C., & Warshaw, D. M. (2007). Hypertrophic and dilated cardiomyopathy mutations differentially affect the molecular force generation of mouse-cardiac myosin in the laser trap assay. *American Journal of Physiology, Heart and Circulatory Physiology*, *293*, 284–291. https://doi.org/10.1152/ajpheart.00128.2007.-Point

Edelberg, J. M., Sehnert, A. J., Mealiffe, M. E., del Rio, C. L., & McDowell, R. (2022). The Impact of Mavacamten on the Pathophysiology of Hypertrophic Cardiomyopathy: A Narrative Review. *American Journal of Cardiovascular Drugs*, 22 (5), 497–510. https://doi.org/10.1007/s40256-022-00532-x

Gollapudi, S. K., Yu, M., Gan, Q. F., & Nag, S. (2021). Synthetic thick filaments: A new avenue for better understanding the myosin super-relaxed state in healthy, diseased, and mavacamten-treated cardiac systems. *Journal of Biological Chemistry*, 296, 100114. https://doi.org/10.1074/jbc.RA120.016506

Gordon, A. M., Regnier, M., & Homsher, E. (2001). Skeletal and Cardiac Muscle Contractile Activation. *News In Physiological Sciences*, *16*, 49–55.

Hypertrophic cardiomyopathy — Symptoms and causes. (2022, December 7). Mayo Clinic. Obtained from https://www.mayoclinic.org/diseases-conditions/hypertrophic-cardiomyopathy/symptoms-causes/syc-20350198

Ingles, J., Burns, C., Bagnall, R. D., Lam, L., Yeates, L., Sarina, T., Puranik, R., Briffa, T., Atherton, J. J., Driscoll, T., & Semsarian, C. (2017). Nonfamilial Hypertrophic Cardiomyopathy. *Circulation: Cardiovascular Genetics*, *10*(2), e001620. https://doi.org/10.1161/CIRCGENETICS.116.001620

Irving, M. (2012). Cell-based studies of the molecular mechanism of muscle contraction. In *Comprehensive Biophysics*, *4*, 191–225. https://doi.org/10.1016/B978-0-12-374920-8.00414-8

Kampourakis, T., & Irving, M. (2015). Phosphorylation of myosin regulatory light chain controls myosin head conformation in cardiac muscle. *Journal of Molecular and Cellular Cardiology*, *85*, 199–206. https://doi.org/10.1016/j.yjmcc.2015.06.002

Keam, S. J. (2022). Mavacamten: First Approval. *Drugs*, *82*(10), 1127–1135. https://doi.org/10.1007/s40265-022-01739-7

Keepers, B., Liu, J., & Qian, L. (2020). What's in a cardiomyocyte – And how do we make one through reprogramming? *Biochimica et Biophysica Acta - Molecular Cell Research*, 1867 (3). https://doi.org/10.1016/j.bbamcr.2019.03.011

Lee, K., Harris, S. P., Sadayappan, S., & Craig, R. (2015). Orientation of myosin binding protein C in the cardiac muscle sarcomere determined by domain-specific immuno-EM. *Journal of Molecular Biology*, *427*(2), 274–286. https://doi.org/10.1016/j.jmb.2014.10.023

Ma, W., Henze, M., Anderson, R. L., Gong, H., Wong, F. L., del Rio, C. L., & Irving, T. (2021). The Super-Relaxed State and Length Dependent Activation in Porcine Myocardium. *Circulation Research*, *129*(6), 617–630. https://doi.org/10.1161/CIRCRESAHA.120.318647

Maron, B. J., Rowin, E. J., & Maron, M. S. (2022). Hypertrophic Cardiomyopathy: New Concepts and Therapies. *Annual Review of Medicine*, *73*, 363–375. https://doi.org/10.1146/annurev-med-042220

McNamara, J. W., Li, A., dos Remedios, C. G., & Cooke, R. (2015). The role of super-relaxed myosin in skeletal and cardiac muscle. *Biophysical Reviews*, *7*(1), 5–14. https://doi.org/10.1007/s12551-014-0151-5

McNamara, J. W., Li, A., Lal, S., Bos, J. M., Harris, S. P., Van Der Velden, J., Ackerman, M. J., Cooke, R., & Dos Remedios, C. G. (2017). MYBPC3 mutations are associated with a reduced super-relaxed state in patients with hypertrophic cardiomyopathy. *PLoS ONE*, *12*(6), e0180064. https://doi.org/10.1371/journal.pone.0180064

McNamara, J. W., Li, A., Smith, N. J., Lal, S., Graham, R. M., Kooiker, K. B., van Dijk, S. J., Remedios, C. G. dos, Harris, S. P., & Cooke, R. (2016). Ablation of cardiac myosin binding protein-C disrupts the super-relaxed state of myosin in murine cardiomyocytes. *Journal of*

Molecular and Cellular Cardiology, *94*, 65–71. https://doi.org/10.1016/j.yjmcc.2016.03.009

McNamara, J. W., Singh, R. R., & Sadayappan, S. (2019). Cardiac myosin binding protein-C phosphorylation regulates the super-relaxed state of myosin. *Proceedings of the National Academy of Sciences of the United States of America*, *116*(24), 11731–11736. https://doi.org/10.1073/pnas.1821660116

Mosqueira, D., Smith, J. G. W., Bhagwan, J. R., & Denning, C. (2019). Modeling Hypertrophic Cardiomyopathy: Mechanistic Insights and Pharmacological Intervention. In *Trends in Molecular Medicine*, 25 (9), 775–790). https://doi.org/10.1016/j.molmed.2019.06.005

Muthu, P., Wang, L., Yuan, C., Kazmierczak, K., Huang, W., Hernandez, O. M., Kawai, M., Irving, T. C., & Szczesna-Cordary, D. (2011). Structural and functional aspects of the myosin essential light chain in cardiac muscle contraction. *The FASEB Journal*, *25*(12), 4394–4405. https://doi.org/10.1096/fj.11-191973

Naber, N., Cooke, R., & Pate, E. (2011). Slow myosin ATP turnover in the super-relaxed state in tarantula muscle. *Journal of Molecular Biology*, *411*(5), 943–950. https://doi.org/10.1016/j.jmb.2011.06.051

Nishimura, R. A., Seggewiss, H., & Schaff, H. V. (2017). Hypertrophic obstructive cardiomyopathy: Surgical myectomy and septal ablation. *Circulation Research*, *121*(7), 771–783. https://doi.org/10.1161/CIRCRESAHA.116.309348

Oakley, C. E., Chamoun, J., Brown, L. J., & Hambly, B. D. (2007). Myosin binding protein-C: Enigmatic regulator of cardiac contraction. *International Journal of Biochemistry and Cell Biology, 39 (12)*, 2161–2166. https://doi.org/10.1016/j.biocel.2006.12.008

Pysz, P., Rajtar-Salwa, R., Smolka, G., Olivotto, I., Wojakowski, W., & Petkow-Dimitrow, P. (2021). Mavacamten - A new disease-specific option for pharmacological treatment of symptomatic patients with hypertrophic cardiomyopathy. *Kardiologia Polska*, 79(9), 949–9954). https://doi.org/10.33963/KP.A2021.0064

Ripa, R. , George, T. , Shumway, K. R. , & Sattar, Y. (2023). *Physiology, Cardiac Muscle* (StatPearls, Ed.). StatPearls. https://www.ncbi.nlm.nih.gov/books/NBK572070/

Rohde, J. A., Roopnarine, O., Thomas, D. D., & Muretta, J. M. (2018). Mavacamten stabilizes an autoinhibited state of two-headed cardiac myosin. *Proceedings of the National Academy of Sciences*, *115*(32). https://doi.org/10.1073/pnas.1720342115

Santiago, C. F., Huttner, I. G., & Fatkin, D. (2021). Mechanisms of TTNtv-related dilated cardiomyopathy: Insights from zebrafish models. *Journal of Cardiovascular Development and Disease*, 8 (2) 1–18). https://doi.org/10.3390/jcdd8020010

Scheid, L. M., Mosqueira, M., Hein, S., Kossack, M., Juergensen, L., Mueller, M., Meder, B., Fink, R. H. A., Katus, H. A., & Hassel, D. (2016). Essential light chain S195 phosphorylation is required for cardiac adaptation under physical stress. *Cardiovascular Research*, *111*(1), 44–55. https://doi.org/10.1093/cvr/cvw066

Schmid, M., & Toepfer, C. N. (2021). Cardiac myosin super relaxation (SRX): A perspective on fundamental biology, human disease and therapeutics. In *Biology Open* (Vol. 10, Issue 2). Company of Biologists Ltd. https://doi.org/10.1242/bio.057646

Spoladore, R., Maron, M. S., D'Amato, R., Camici, P. G., & Olivotto, I. (2012). Pharmacological treatment options for hypertrophic cardiomyopathy: high time for evidence. *European heart journal, 3*3 (14), 1724–1733. https://doi.org/10.1093/eurheartj/ehs150

Squire, J. (2019). Special issue: The actin-myosin interaction in muscle: Background and overview. *International Journal of Molecular Sciences, 20 (22).* https://doi.org/10.3390/ijms20225715

Toepfer, C. N., Garfinkel, A. C., Venturini, G., Wakimoto, H., Repetti, G., Alamo, L., Sharma, A., Agarwal, R., Ewoldt, J. F., Cloonan, P., Letendre, J., Lun, M., Olivotto, I., Colan, S., Ashley, E., Jacoby, D., Michels, M., Redwood, C. S., Watkins, H. C., … Seidman, C. E. (2020). Myosin Sequestration Regulates Sarcomere Function, Cardiomyocyte Energetics, and Metabolism, Informing the Pathogenesis of Hypertrophic Cardiomyopathy. *Circulation*, 828–842. https://doi.org/10.1161/CIRCULATIONAHA.119.042339

Toepfer, C. N., Wakimoto, H., Garfinkel, A. C., McDonough, B., Liao, D., Jiang, J., Tai, A. C., Gorham, J. M., Lunde, I. G., Lun, M., Lynch, T. L., McNamara, J. W., Sadayappan, S., Redwood, C. S., Watkins, H. C., Seidman, J. G., & Seidman, C. E. (2019). Hypertrophic cardiomyopathy mutations in MYBPC3 dysregulate myosin. *Science Translational Medicine*, *11*(476). https://doi.org/10.1126/scitranslmed.aat1199

Voorhees, A. P., & Han, H. C. (2015). Biomechanics of cardiac function. *Comprehensive Physiology*, *5*(4), 1623–1644. https://doi.org/10.1002/cphy.c140070

8. Appendix

Appendix 1 – Ethical Approval

Region Hovedstaden

Center for Sundhed

De Videnskabsetiske Komiteer

Borgervænget 3, stuen
2100 København Ø

Telefon 3866 6395
Mail vek@regionh.dk

Journal-nr.: F-22041953

Dato: 10-10-2022

Maria Helena Dominguez Vall-Lamora
Frederiksberg Hospital
Kardiologisk afdeling Y
Nordre Fasanvej 57
2000 Frederiksberg

F-22041953 Forespørgsel om anmeldelsespligt til videnskabsetisk komite

Projekt: Analyse af muskelvæv efter operation for fortykket hjertemuskel, hvor der fjernes et stykke af hjertets skillevæg.

Du har ved mail af 19. juli 2022 spurgt, om ovennævnte projekt skal anmeldes til det videnskabsetiske komitesystem.

Det er vurderet, at der ikke er tale om et sundhedsvidenskabeligt forskningsprojekt som dette er defineret i komitélovens § 2[1],da det er oplyst, at projektet alene undersøger fuldt anonymiseret biologisk materiale.

Projektet er derfor ikke anmeldelsespligtigt jf. komitélovens § 1, stk. 4 og kan iværksættes uden tilladelse fra De Videnskabsetiske Komiteer for Region Hovedstaden.

I Danmark har det videnskabsetiske komitesystem til opgave at vurdere sundhedsvidenskabelige og sundhedsdatavidenskabelige forskningsprojekter.

Ved sundhedsvidenskabelige forskningsprojekter forstås projekter, der indebærer forsøg på levendefødte menneskelige individer, menneskelige kønsceller, der agtes anvendt til befrugtning, menneskelige befrugtede æg, fosteranlæg og fostre, væv, celler og arvebestanddele fra mennesker, fostre og lign. eller afdøde. Herunder omfattes kliniske forsøg med lægemidler på mennesker og klinisk afprøvning af medicinsk udstyr.

Sundhedsvidenskabelig forskning omhandler primært forskning inden for de lægevidenskabelige fag, den kliniske og den socialmedicinsk-epidemiologiske forskning. Begrebet omfatter udover forskning af de somatiske sygdomme, tillige de psykiatriske og de klinisk-psykologiske sygdomme og tilstandsformer. Herudover inddrages tilsvarende odontologisk og farmaceutisk forskning under begrebet.

[1] Afgørelsen er truffet efter lov lovbekendtgørelse nr. 1083 af 15/09/2017 med senere ændringer

Registerforskningsprojekter (bortset fra sundhedsdatavidenskabelige projekter), interviewundersøgelser og spørgeskemaundersøgelser skal kun anmeldes, hvis der indgår menneskeligt biologisk materiale i projektet.

Undersøgelser af anonymt biologisk humant materiale skal dog ikke anmeldes til en videnskabsetisk komite, med mindre der er tale om et forskningsprojekt vedrørende befrugtede menneskelige æg samt kønsceller, jf. §§ 25 og 27, stk. 2 i lov om kunstig befrugtning i forbindelse med lægelig behandling, diagnostik og forskning m.v. Det er et krav, at materiale er fuldstændig anonymt (der må ikke være en identifikationskode til data), og at materialet er indsamlet i overensstemmelse med lovgivningen på indsamlingsstedet.
Forsøg på cellelinjer eller lignende, der stammer fra et forsøg med indsamling af celler eller væv, som har opnået den nødvendige godkendelse, skal heller ikke anmeldes.

Forsøg, der alene har til formål at fastlægge et kemikaliums toksikologiske grænse i mennesket, er ikke anmeldelsespligtige. Ved et kemikalium forstås i denne forbindelse et stof, der ikke finder terapeutisk anvendelse.

Der ligger i afvisningen af at bedømme projektet ikke nogen etisk stillingtagen eller negativ vurdering af dets indhold.

Ved sundhedsdatavidenskabelige forskningsprojekter forstås forskning vedrørende særlige komplekse områder i afledte sensitive bioinformatiske data frembragt ved omfattende kortlægning af arvemassen eller billeddiagnostik i forbindelse med forsøg eller klinisk diagnostik af patienter.

Vi gør opmærksom på, at regionerne i visse tilfælde skal godkende videregivelse af oplysninger fra patientjournaler. Det er den region, forsker er ansat i, der skal ansøges om dette. Nærmere oplysninger kan findes på den relevante regions hjemmeside.

Behandling af personhenførbare oplysninger er omfattet af databeskyttelsesloven/databeskyttelsesforordningen. Nærmere oplysning herom findes på Datatilsynets hjemmeside.

Klagevejledning

Afgørelsen kan, jf. komitélovens § 26, stk. 1, indbringes for National Videnskabsetisk Komité, senest 30 dage efter afgørelsen er modtaget. National Videnskabsetisk Komité kan, af hensyn til sikring af forsøgspersonernes rettigheder, behandle elementer af projektet, som ikke er omfattet af selve klagen.

Klagen skal indbringes elektronisk og ved brug af digital signatur og kryptering, hvis protokollen indeholder fortrolige oplysninger. Dette kan ske på adressen: dketik@dketik.dk.

Klagen skal begrundes og være vedlagt kopi af Den Regionale Videnskabsetiske Komités afgørelse samt de sagsakter, som Den Regionale Videnskabsetiske Komité har truffet afgørelse på grundlag af.

NB: Der må ikke foretages ændringer i dokumenterne, som har været til behandling i komiteen, da sagen ellers vil blive sendt retur til komiteen.

Databeskyttelse - fortegnelseskrav
Du skal være opmærksom på, at du kan være forpligtet til at få forskningsprojektet fortegnet.

Er du forsker ansat i Region Hovedstaden, gør du dette ved at rette henvendelse til Videnscenter for Dataanmeldelser i Region Hovedstaden, som er den regionale enhed, der administrerer forskningsfortegnelsen. Du kan læse mere om fortegnelsen og finde kontaktoplysninger på videnscenterets hjemmeside.

Er du ikke ansat i Region Hovedstaden, kan du orientere dig om fortegnelseskravet i Vejledning om fortegnelse på Datatilsynets hjemmeside.

Med venlig hilsen

Anne Brunsgaard
konsulent

Appendix 2 – Solutions Used For The Mant-ATP Chase Experiment

1. Relaxing solution

Compounds	250 ml
KCL	10 mL
Imidazol	5 mL
MgCl2	2.5 mL
EGTA	5 mL
ATP	0.625 g

2. TCEP

TCEP stock at 100 mM, use at 1:100

Compounds	Volume
TCEP	0.144 g
dH2O	5 ml
pH to 6.8	

3. ATP

ATP at 500 mM, use 1:100 (glycerinating solution) and 1:125 (ATP chase buffer)

Compounds	Volume
ATP	1,378 g
dH2O	5 ml
pH to 6.8	

4. Stock solution MYK-461

The following equation was used to calculate the amount of MYK-461 that needed to be weighed and dissolved into 2 mL DMSO.

$$Mass = Concentration * Volume * Molecular\ weight$$

$$Mass = 1\ mM * 2\ mL * 273{,}33 \frac{g}{mol}$$

$$Mass = 0{,}001 \frac{mol}{L} * 0{,}002\ L * 273.330 \frac{mg}{mol}$$

$$Mass = 0{,}5466\ mg$$

A dilution equation was used to calculate how much MYK-461 was needed to get 1 µM.

$$V_{before} * C_{before} = V_{after} * C_{after}$$

$$2\ mL * 1\ mM = V_{after} * 1\ \mu M$$

$$2\ mL * 0{,}001\ \mu M = V_{after} * 1\ \mu M$$

$$\frac{2\ mL * 0{,}001\ \mu M}{1\ \mu M} = V_{after}$$

$$0{,}002\ mL = 2\ \mu L = V_{after}$$

5. Rigor buffer with 1 µM MYK-461

Common buffer + EGTA	2 mL
MYK-461	2 µL
TCEP	20 µL

6. ATP-Chase buffer with 1 µM MYK-461

Common buffer + EGTA	530.4 µL
MYK-461	0.5304 µL
TCEP	5.4 µL
ATP	4.32 L

7. Mant-ATP buffer with 1 µM MYK-461

Common buffer + EGTA	507.6 µl
MYK-461	0.5076 µL
TCEP	5.4 µL
Mant-ATP	27 µL

Appendix 3 – Materials

Reagent type	Designation	Source of reference	Identifier	Additional information
Drug	MYK-461 / Mavacamten	Cayman Chemical Company	Cat#19216	Soluble in DMSO
Fluorescent reagent	Mant-ATP, trisodium salt	Invitrogen by Thermo Fisher Scientific	Cat#M12417	Stored at -20°C
Liquid	Glycerol	Honeywell	Cat#15523-1L	Stored at 25 °C
Grids	Copper mesh/ Copper grids	SPI supplies	Cat#2010C-XA	For electron microscopy and to mount cardiac strips
Microscope slide	Superfrost Plus Adhesion Microscope Slides White tap	Epredia	Cat#J1800AMNZ	75 mm x 25 mm
Cover slips	Cover Slips	Epredia	Cat# BB02400240AC53MNZ0	24 mm x 24 mm
Solid chemical compound	ATP, ATP magnesium salt	Sigma-Aldrich (Merck)	Cat#74804-12-9	Stored at -20 °C

Appendix 4 - Buffers For Mant-ATP Chase Experiment

1. Common buffer - 1 liter (pH 6.8)

	Concentration (mM)	Molecular weight (Mw)	Mass to add (g) / 1 liter
K acetate	120	98.14	11.78
Mg Acetate (tetrahydrate)	5	214.45	1.07
K2HPO4 (Potassium phosphate, dibasic)	2.5	174.18	0.435
KH2PO4 (Potassium phosphate, monobasic)	2.5	136.09	0.34
MOPS	50	209.26	10.46
pH to 6.8 with 10 M KOH			

2. Rigor Buffer - for 6 fibers

Common buffer + EGTA	2 mL
TCEP	20 µL

3. Mant-ATP buffer - for 6 fibers

Common buffer + EGTA	507.6 µl
TCEP	5.4 µL
MANT-ATP	27 µL

4. ATP chase buffer - for 6 fibers

Common buffer + EGTA	530.4 µL
TCEP	5.4 µL
ATP	4.32 µL